Electronic Supplementary Material (ESI) for Journal of Materials Chemistry A.

Supporting Information

Oxygen-Vacancy Rich $Ir_xMo_{1-x}O_y$ Nanofibers for Oxygen Evolution Reaction: pH-Universal and Electrolyte-Concentration Independent Excellent Catalytic Activity

Sung Hwa Ahn,[1] Dasol Jin,[1] Chongmok Lee, Youngmi Lee*

Department of Chemistry & Nanoscience, Ewha Womans University, Seoul 03760, Republic of Korea

[1]Equally contributed to this work

*Corresponding author: youngmilee@ewha.ac.kr (Y. L.)

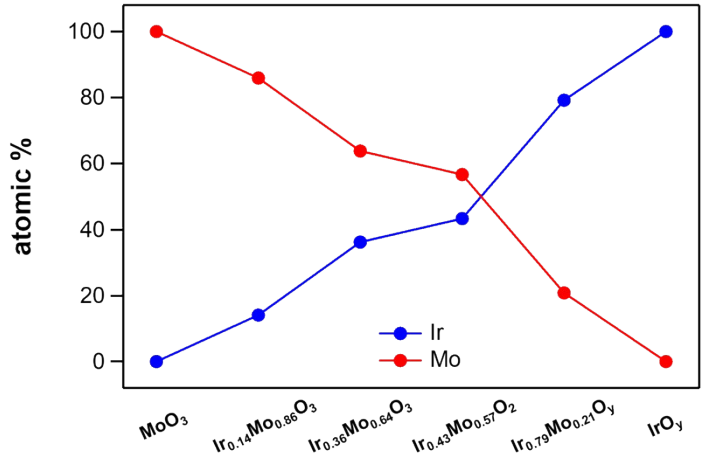

Fig. S1. Relative atomic percentages of Ir and Mo in the $Ir_xMo_{1-x}O_y$ samples determined with EDS analysis. The values were calculated by averaging the EDS spectra collected from 10 different areas for each sample and were tabulated in Table S1.

Table S1. Comparison of atomic percentages of the $Ir_xMo_{1-x}O_y$ samples determined with EDS analysis.

Sample	Ir (*at*.%)	Mo (*at*.%)
$Ir_{0.14}Mo_{0.86}O_3$	14.07 (± 1.29)	85.93 (± 1.29)
$Ir_{0.36}Mo_{0.64}O_3$	36.25 (± 1.42)	63.75 (± 1.42)
$Ir_{0.43}Mo_{0.57}O_2$	43.37 (± 0.70)	56.63 (± 0.70)
$Ir_{0.79}Mo_{0.21}O_y$	79.14 (± 2.51)	20.86 (± 2.51)

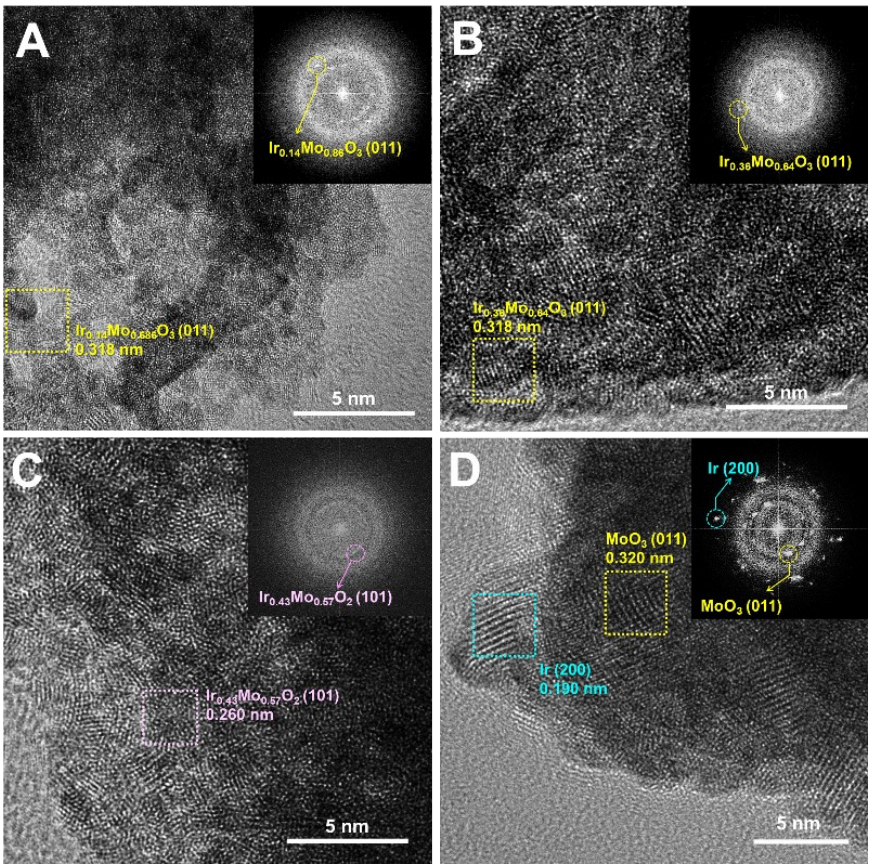

Fig. S2. High-resolution TEM images of (A) $Ir_{0.14}Mo_{0.86}O_3$, (B) $Ir_{0.36}Mo_{0.64}O_3$, (C) $Ir_{0.43}Mo_{0.57}O_2$, and (D) $Ir_{0.79}Mo_{0.21}O_y$. Insets: corresponding FFT patterns.

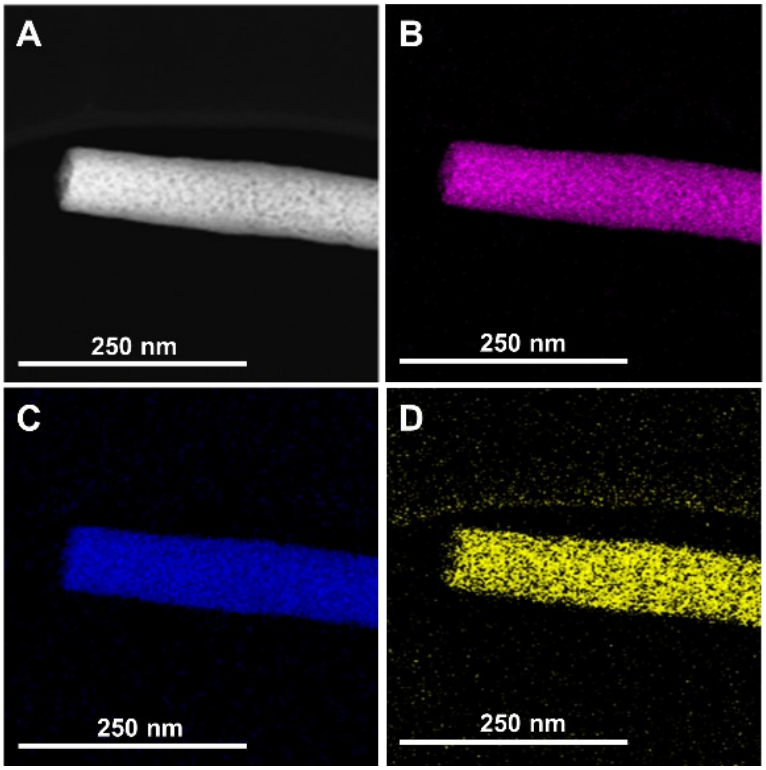

Fig. S3. (A) Representative TEM image and (B-D) elemental mapping images of $Ir_{0.43}Mo_{0.57}O_2$. Pink, blue and yellow colors correspond to the elements of Ir, Mo and O, respectively.

Table S2. Accurate Ir 4f peak positions obtained from XPS peaks in Fig. 4A.

Catalyst			$Ir_{0.43}Mo_{0.57}O_2$	IrO_y
Ir 4f	$4f_{7/2}$	Ir^{4+}	62.18	61.63
		Ir^{3+}	62.88	62.58
		Ir	-	60.88
	$4f_{5/2}$	Ir^{4+}	65.18	64.58
		Ir^{3+}	66.08	65.63
		Ir	-	63.68

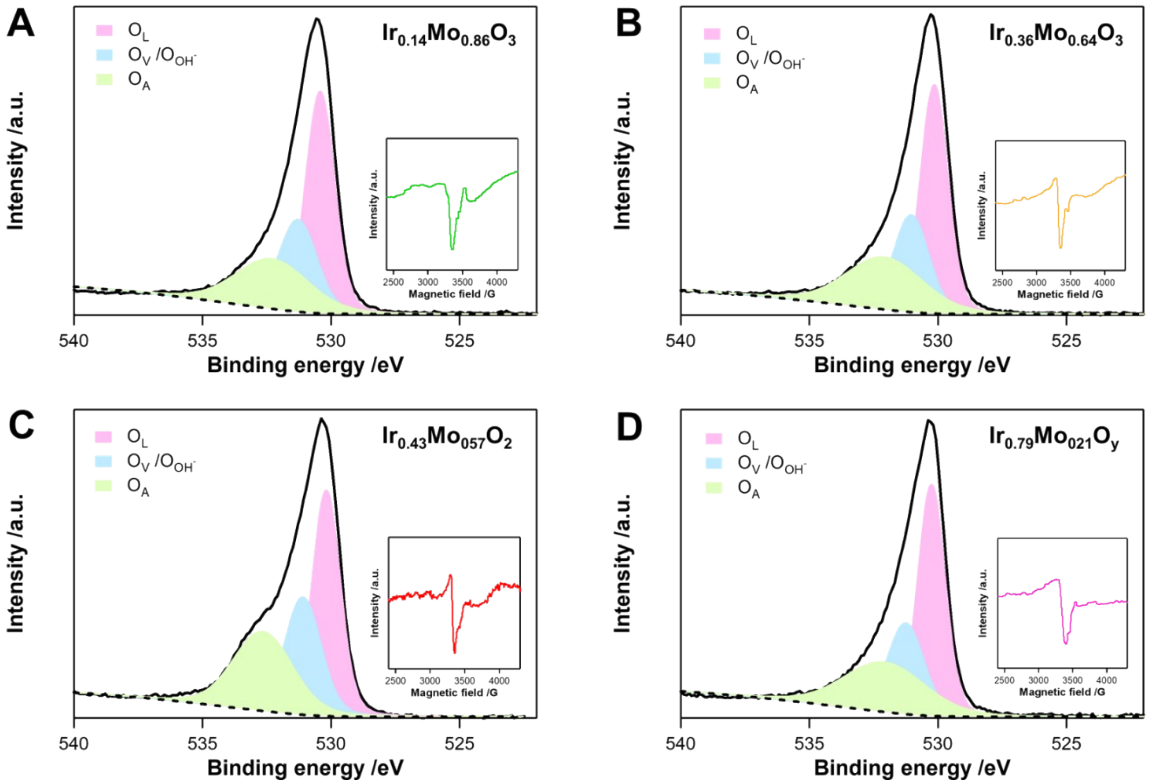

Fig. S4. Deconvoluted O 1s XPS spectra of $Ir_xMo_{1-x}O_y$ nanomaterials ($0 < x < 1$). Insets: corresponding EPR spectra.

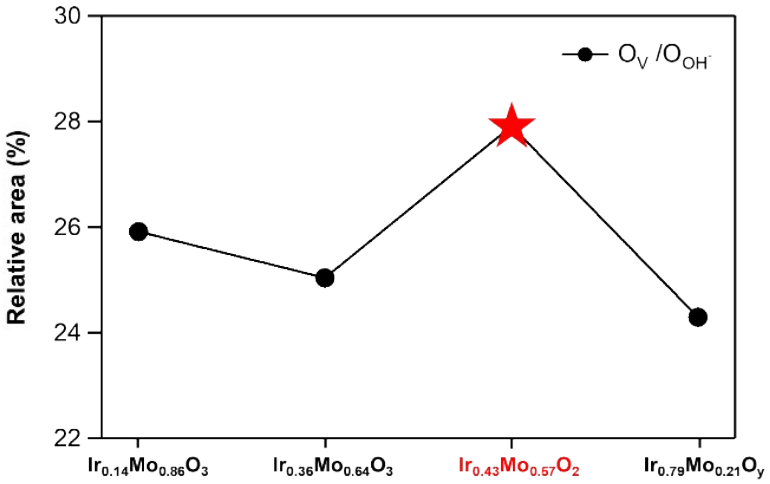

Fig. S5. Relative XPS peak area associated with surface hydroxyl oxygen (O_V/O_{OH-}) out of total peak area in O 1s region for $Ir_xMo_{1-x}O_y$ ($0 < x < 1$) nanomaterials.

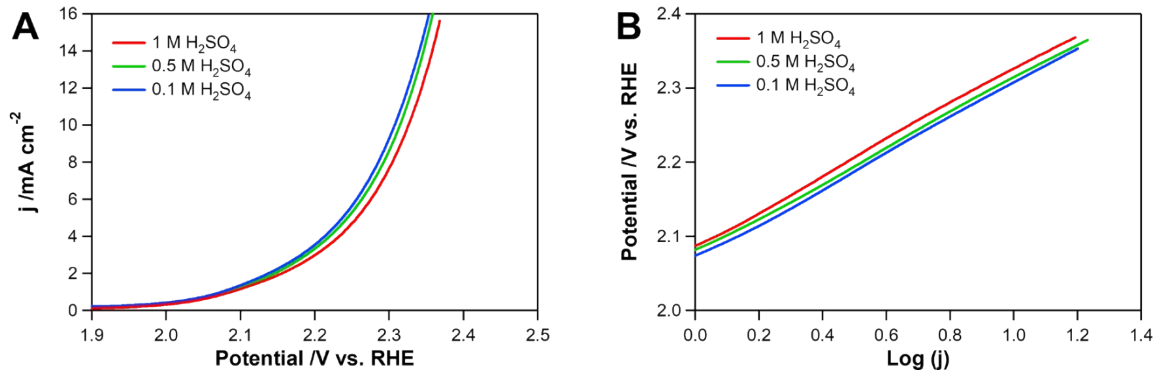

Fig. S6. (A) Polarization curves for OER at 1 mV s^{-1} on the catalysts of MoO_3 in H_2SO_4 solutions and (B) the corresponding Tafel plots derived from the LSVs.

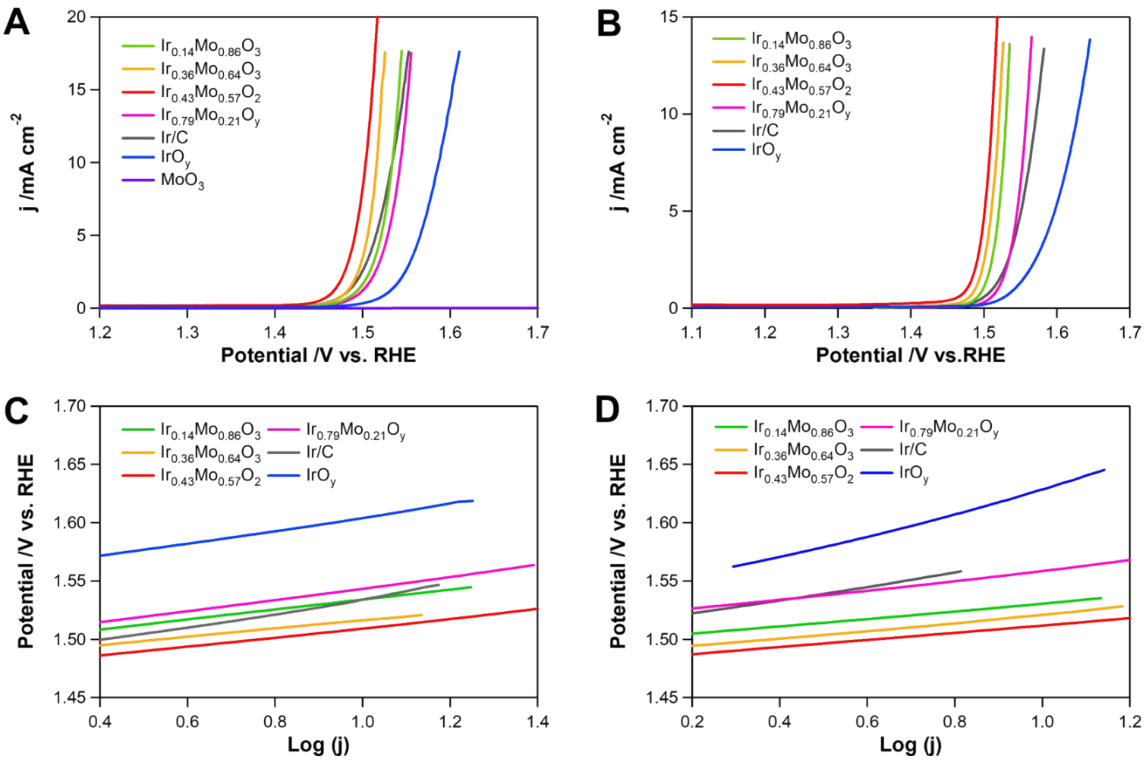

Fig. S7. (A,B) Polarization curves of as-prepared $Ir_xMo_{1-x}O_y$ series, IrO_y and Ir/C measured in Ar-saturated 0.5 M aqueous electrolytes at a scan rate of 1 mV s^{-1} and a rotating speed of 1600 rpm. (C,D) Corresponding Tafel plots derived from the LSVs. The measurements were performed in 0.5 M solutions of (A,C) H_2SO_4, (B,D) KOH.

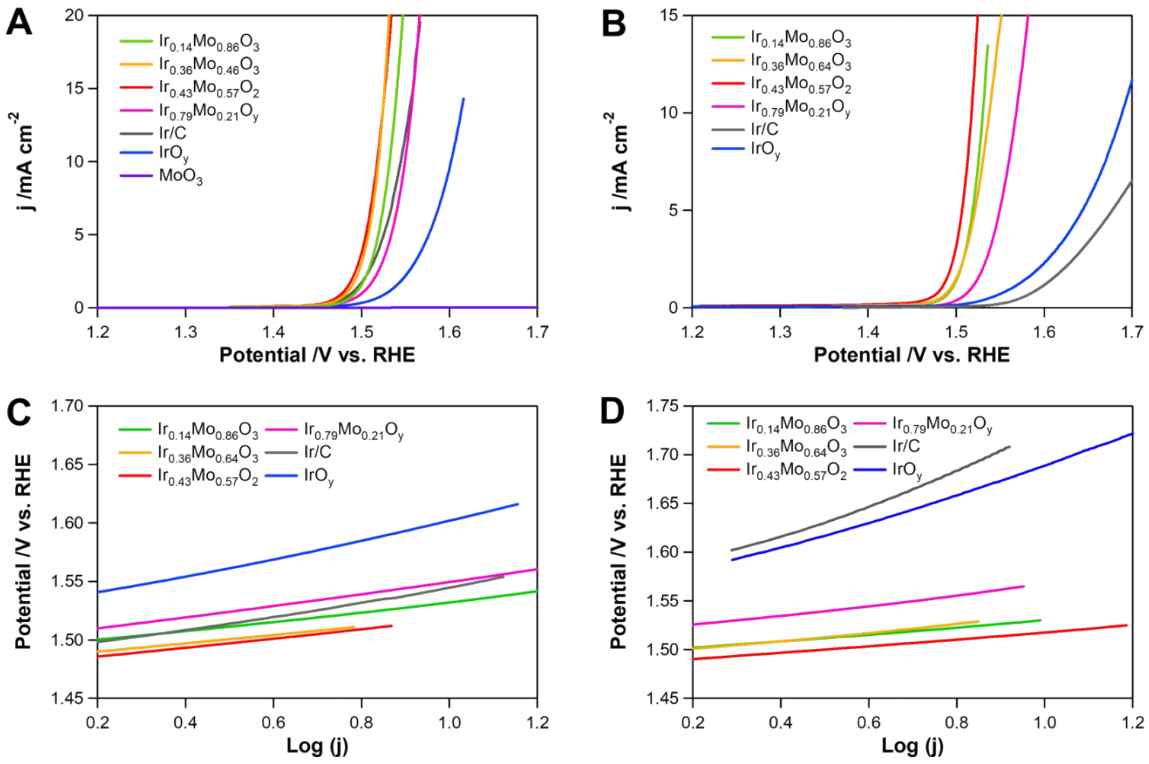

Fig. S8. (A,B) Polarization curves of as-prepared $Ir_xMo_{1-x}O_y$ series, IrO_y and Ir/C measured in Ar-saturated 0.1 M aqueous electrolytes at a scan rate of 1 mV s^{-1} and a rotating speed of 1600 rpm. (C,D) Corresponding Tafel plots derived from the LSVs. The measurements were performed in 0.1 M solutions of (A,C) H_2SO_4 and (B,D) KOH.

Table S3. Comparison of potential (V *vs*. RHE) at current density of 10 mA cm^{-2} of $Ir_xMo_{1-x}O_y$ series, single metal oxides (IrO_y and MoO_3) and Ir/C as a function of pH varied with different electrolyte concentrations.

Catalyst / pH (electrolyte)	$Ir_{0.14}Mo_{0.86}O_3$	$Ir_{0.36}Mo_{0.64}O_3$	**$Ir_{0.43}Mo_{0.57}O_2$**	$Ir_{0.79}Mo_{0.21}O_y$	Ir/C	IrO_y	MoO_3
0 (1 M H_2SO_4)	1.538	1.530	**1.500**	1.541	1.538	1.574	2.326
0.3 (0.5 M H_2SO_4)	1.535	1.517	**1.504**	1.544	1.540	1.587	2.315
1 (0.1 M H_2SO_4)	1.532	1.519	**1.517**	1.549	1.547	1.601	2.308
7.1 (1 M PBS)	1.536	1.517	**1.507**	1.591	1.581	1.687	-
13 (0.1 M KOH)	1.531	1.538	**1.518**	1.568	1.747	1.689	-
13.7 (0.5 M KOH)	1.530	1.521	**1.512**	1.558	1.571	1.629	-
14 (1 M KOH)	1.530	1.520	**1.515**	1.557	1.548	1.617	-

Table S4. Comparison of Tafel slope (mV dec^{-1}) of $Ir_xMo_{1-x}O_y$ series, single metal oxides (IrO_y and MoO_3) and Ir/C as a function of pH varied with different electrolyte concentrations.

Catalyst / pH (electrolyte)	$Ir_{0.14}Mo_{0.86}O_3$	$Ir_{0.36}Mo_{0.64}O_3$	**$Ir_{0.43}Mo_{0.57}O_2$**	$Ir_{0.79}Mo_{0.21}O_y$	Ir/C	IrO_y	MoO_3
0 (1 M H_2SO_4)	50.2	41.6	**39.0**	49.6	56.3	54.8	240
0.3 (0.5 M H_2SO_4)	43.6	38.3	**38.1**	48.1	56.1	58.2	234
1 (0.1 M H_2SO_4)	40.0	38.9	**38.8**	49.9	59.0	70.1	238
7.1 (1 M PBS)	49.4	41.7	**41.5**	75.7	95.0	118	-
13 (0.1 M KOH)	34.6	40.3	**34.5**	51.4	171	149	-
13.7 (0.5 M KOH)	32.1	33.2	**31.7**	40.6	57.2	98.2	-
14 (1 M KOH)	30.7	30.8	**30.6**	38.2	50.5	75.4	-

Table S5. Comparison of mass activities of the samples under the different pH values of 1 M solutions.

Catalyst	Mass activity (mA mg_{Ir}^{-1})		
	H_2SO_4	PBS (pH 7.1)	KOH
$Ir_{0.14}Mo_{0.86}O_3$	52.51	64.56	30.57
$Ir_{0.36}Mo_{0.64}O_3$	61.83	78.92	66.10
$Ir_{0.43}Mo_{0.57}O_2$	127.8	134.4	143.4
$Ir_{0.79}Mo_{0.21}O_y$	40.12	16.89	9.912
Ir/C	129.5	96.48	52.54

Table S6. Comparison of turnover frequency (TOF) values of $Ir_xMo_{1-x}O_y$ materials ($0 < x < 1$) in 1 M H_2SO_4, 1 M PBS (pH 7.1) and 1 M KOH solutions. Each TOF calculation was specifically performed at a potential of 1.53 V (*vs*. RHE).

Solution	Sample	TOF (s^{-1})
1 M H_2SO_4	$Ir_{0.14}Mo_{0.86}O_3$	0.013
	$Ir_{0.36}Mo_{0.64}O_3$	0.013
	$Ir_{0.43}Mo_{0.57}O_2$	**0.047**
	$Ir_{0.79}Mo_{0.21}O_y$	0.006
1 M PBS (pH 7.1)	$Ir_{0.14}Mo_{0.86}O_3$	0.013
	$Ir_{0.36}Mo_{0.64}O_3$	0.014
	$Ir_{0.43}Mo_{0.57}O_2$	**0.028**
	$Ir_{0.79}Mo_{0.21}O_y$	0.002
1 M KOH	$Ir_{0.14}Mo_{0.86}O_3$	0.016
	$Ir_{0.36}Mo_{0.64}O_3$	0.018
	$Ir_{0.43}Mo_{0.57}O_2$	**0.041**
	$Ir_{0.79}Mo_{0.21}O_y$	0.002

Turnover frequency (TOF) is a straightforward intrinsic activity marker that can demonstrate how efficient an electrocatalyst is for the reaction of interest with determining the exact number of active sites participating in the catalysis.

The turnover frequency (TOF) was calculated using following equation:

TOF = (Generated number of O_2 molecules)/(Number of metal sites)

where the generated number of O_2 molecules is obtained from the measured current density (*j*) and surface area of the metal oxide (A), according to the following equation:

$$\text{Number of } O_2 \text{ molecules} = \left(j\ \frac{mA}{cm^2}\right)\left(A\ cm^2\right)\left(\frac{1\ \frac{C}{s}}{1000\ mA}\right)\left(\frac{1\ mol\ e^-}{96{,}485\ C}\right)\left(\frac{1\ mol\ O_2}{4\ mol\ e^-}\right)\left(\frac{6.02\ \times\ 10^{23}\ O_2}{1\ mol\ O_2}\right)$$

where the number of metal sites is the number of loaded Ir atoms on the electrode.

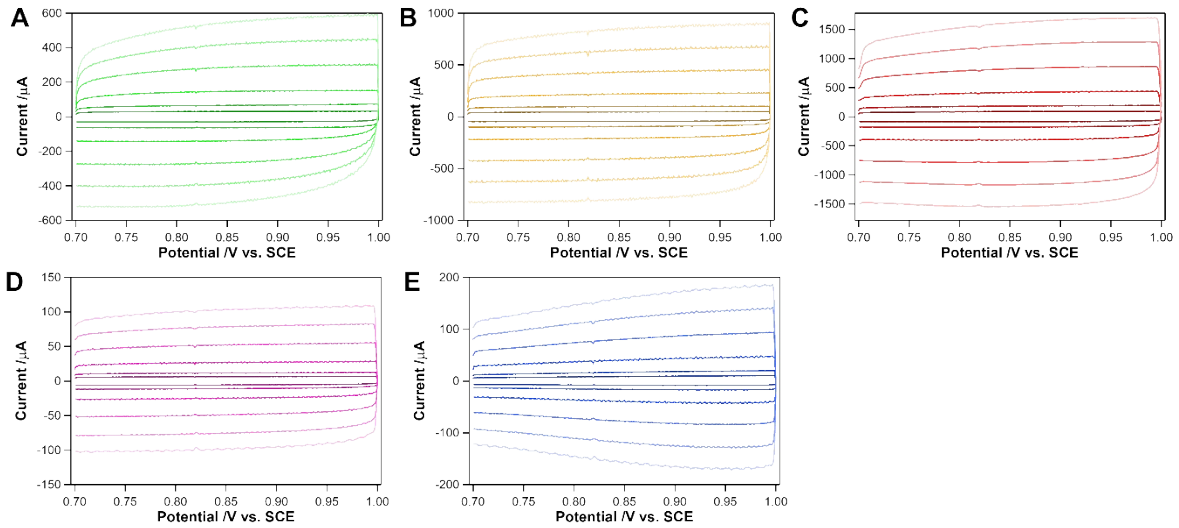

Fig. S9. Cyclic voltammograms of (A) $Ir_{0.14}Mo_{0.86}O_3$, (B) $Ir_{0.36}Mo_{0.64}O_3$, (C) $Ir_{0.43}Mo_{0.57}O_2$, (D) $Ir_{0.79}Mo_{0.21}O_y$ and (E) IrO_y in 1 M H_2SO_4 solution (*aq*) at various scan rates (10, 20, 50, 100, 150 and 200 mV s^{-1}).

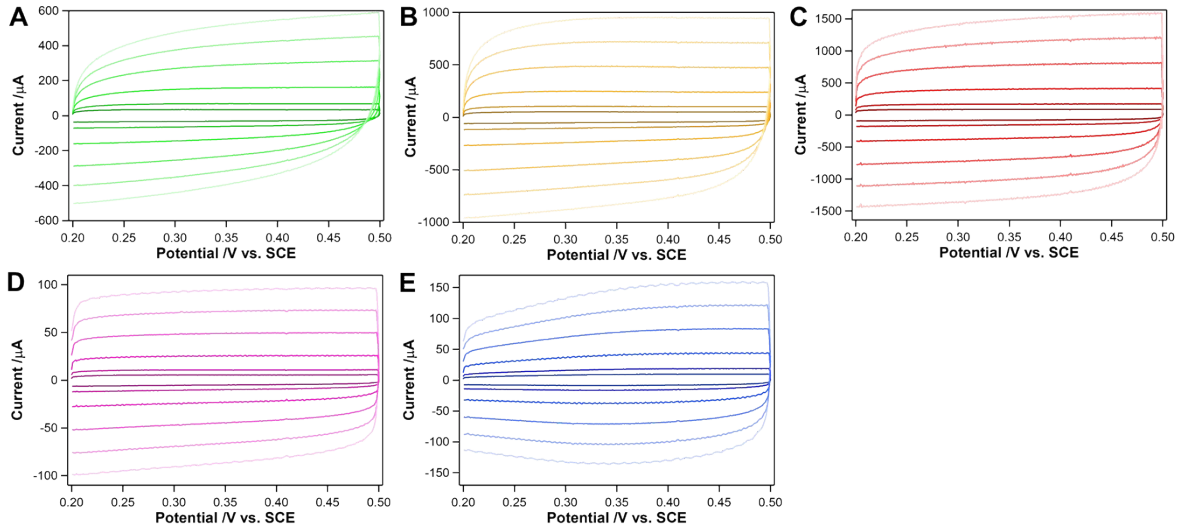

Fig. S10. Cyclic voltammograms of (A) $Ir_{0.14}Mo_{0.86}O_3$, (B) $Ir_{0.36}Mo_{0.64}O_3$, (C) $Ir_{0.43}Mo_{0.57}O_2$, (D) $Ir_{0.79}Mo_{0.21}O_y$ and (E) IrO_y in 1 M PBS (*aq*, pH 7.1) at various scan rates (10, 20, 50, 100, 150 and 200 mV s^{-1}).

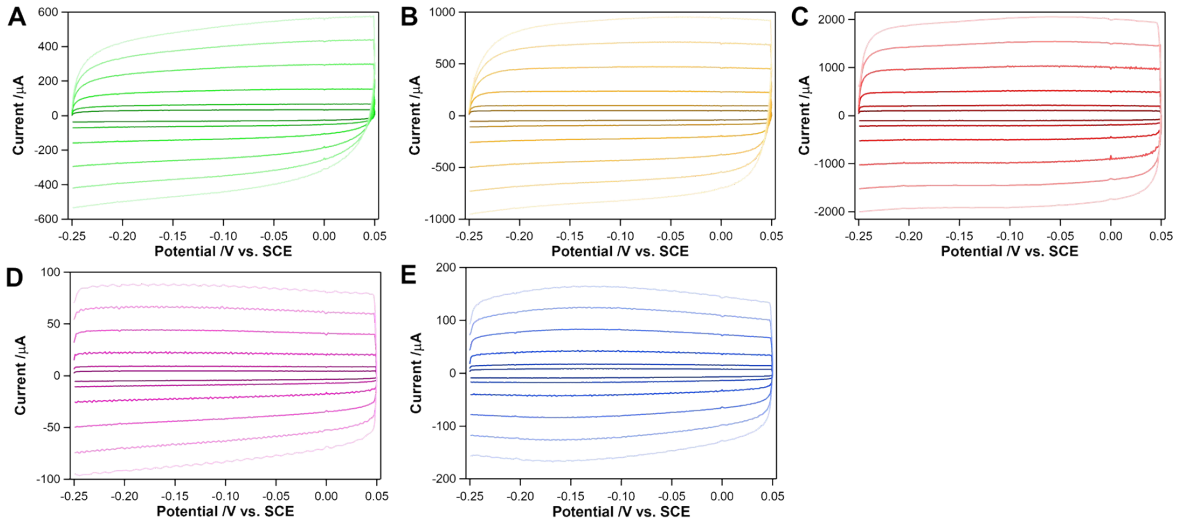

Fig. S11. Cyclic voltammograms of (A) $Ir_{0.14}Mo_{0.86}O_3$, (B) $Ir_{0.36}Mo_{0.64}O_3$, (C) $Ir_{0.43}Mo_{0.57}O_2$, (D) $Ir_{0.79}Mo_{0.21}O_y$ and (E) IrO_y in 1 M KOH solution (*aq*) at various scan rates (10, 20, 50, 100, 150 and 200 mV s^{-1}).

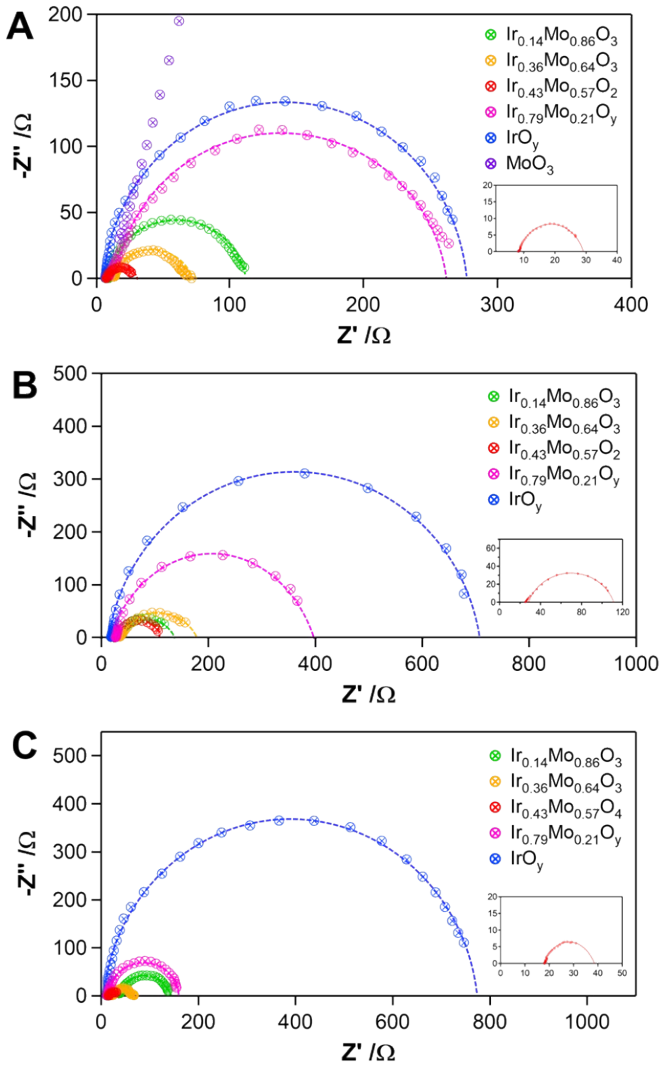

Fig. S12. Nyquist plots of various nanomaterials at 1.54 V (*vs*. RHE) in (A) 1 M H_2SO_4, (B) 1 M PBS (pH 7.1), and (C) 1 M KOH solutions. Insets: enlarge plots along the *x*-axis for

Table S7. Comparison of the charge transfer resistance values for the $Ir_xMo_{1-x}O_y$ samples under acidic, neutral and alkaline conditions.

Catalysts	Resistance (Ω)		
	1 M H_2SO_4	1 M PBS	1 M KOH
$Ir_{0.14}Mo_{0.86}O_3$	102.1	114.6	111.0
$Ir_{0.36}Mo_{0.64}O_3$	63.61	136.8	56.91
$Ir_{0.43}Mo_{0.57}O_2$	**24.26**	**80.38**	**40.65**
$Ir_{0.79}Mo_{0.21}O_y$	244.1	381.5	145.1
IrO_y	267.8	688.9	756.1

Table S8. Comparison of OER activities (*i.e.*, Tafel slopes and potential at 10 mA cm^{-2}) of $Ir_{0.43}Mo_{0.57}O_2$ and other previously reported Ir-based electrocatalysts under the aqueous solutions with various pH values.

Catalysts	Solution	Potential at 10 mA cm^{-2} (V vs. RHE)	Tafel slope (mV dec^{-1})	ref
$Ir_{0.43}Mo_{0.57}O_2$	**1 M H_2SO_4**	**1.505**	**39**	This work
$Ir_{0.43}Mo_{0.57}O_2$	**0.5 M H_2SO_4**	**1.506**	**38.1**	This work
[a]$IrMoO_x$	0.5 M H_2SO_4	1.497	46.1	[31]
[b]P-IrO_x@DG	0.5 M H_2SO_4	1.521	67.5	[48]
[c]Ir-MoO_3	0.5 M H_2SO_4	1.386	48	[58]
[d]BPIr-be	0.5 M H_2SO_4	1.52	64	[49]
[e]$Y_2Ru_{1.2}Ir_{0.8}O_7$	0.5 M H_2SO_4	1.45	47.56	[50]
[f]$Ir_{0.48}Cu_{0.52}O_y$	0.5 M H_2SO_4	1.488	40.6	[33]
$Ir_{0.43}Mo_{0.57}O_2$	**0.1 M H_2SO_4**	**1.520**	**38.8**	This work
[g]Ir-NSG	0.1 M $HClO_4$	1.495	44.2	[51]
[h]$IrO_2/LiLa_2IrO_6$	0.1 M $HClO_4$	1.522	39.2	[52]
[j]Ru@IrO_x	0.05 M H_2SO_4	1.512	69.1	[57]
[i]IM-30	0.1 M $HClO_4$	1.68 (j=25.2)	57	[59]
$Ir_{0.43}Mo_{0.57}O_2$	**1 M PBS**	**1.496**	**41.5**	This work
[b]P-IrO_x@DG	1 M PBS	1.570	106.4	[48]
[f]$Ir_{0.48}Cu_{0.52}O_y$	1 M PBS	1.558	68.2	[33]
[g]Ir-NSG	1 M PBS	1.537	74.2	[51]
[d]BPIr-be	PBS (pH=7)	1.85	70	[49]
$Ir_{0.43}Mo_{0.57}O_2$	**1 M KOH**	**1.506**	**30.6**	This work
[b]P-IrO_x@DG	1 M KOH	1.478	52.8	[48]
[k]$Ir/Ni(OH)_2$	1 M KOH	1.454	41	[53]
[f]$Ir_{0.48}Cu_{0.52}O_y$	1 M KOH	1.517	37.1	[33]
[l]Ir_{SA}-Ni_2P	1 M KOH	1.379	90.1	[54]
[m]Ir/CoNiB	1 M KOH	1.408	35.1	[55]
[g]Ir-NSG	1 M KOH	1.486	39.9	[51]
[d]BPIr-be	1 M KOH	1.52	70	[49]
$Ir_{0.43}Mo_{0.57}O_2$	**0.5 M KOH**	**1.505**	**31.7**	This work
$Ir_{0.43}Mo_{0.57}O_2$	**0.1 M KOH**	**1.508**	**34.5**	This work
[n]$SrIrO_3$	0.1 M KOH	1.530	42	[56]

[(i)]IM-30	0.1 M NaOH	1.73 (j = 22.2)	-	[59]

[(a)]$IrMoO_x$ represents nanofibers distributed the two components of MoO_x and IrO_x; [(b)]P-IrO_x@DG represents porous IrO_x nanoclusters supported on defective graphene (DG); [(c)]Ir-MoO_3 represents semiconducting metal oxides consisting of Ir and MoO_3 embedded by graphitic carbon layers; [(d)]BPIr-be represents exposed 2D black phosphorus (BP) nanosheets by coating the Ir nanoparticle on the carbon cloth (CC) substrate and then the BP nanosheets on the top; [(e)]$Y_2Ru_{1.2}Ir_{0.8}O_7$ represents iridium doped yttrium ruthenate pyrochlore catalysts; [(f)]$Ir_{0.48}Cu_{0.52}O_y$ represents nanotube that Cu is inserted within IrO_2; [(g)]Ir-NSG represents iridium nanoclusters embedded on nitrogen and sulfur co-doped graphene; [(h)]$IrO_2/LiLa_2IrO_6$ represents $LiLa_2IrO_6$ electrocatalyst with a thin IrO_2 shell; [(i)]IM-30 represents iridium-based molybdenum mixed oxide composites; [(j)]Ru@IrO_x represents a core-shell RuIr nanostructure with a highly strained and disordered Ru core and a partially oxidized Ir shell; [(k)]$Ir/Ni(OH)_2$ represents Ir nanoparticles anchored on the $Ni(OH)_2$ nanosheets; [(l)]Ir_{SA}-Ni_2P represents an iridium single atom on Ni_2P catalyst; [(m)]Ir/CoNiB represents iridium clusters decorated on CoNiB (amorphous metal borides); [(n)]$SrIrO_3$ represents perovskite oxide in a monoclinic structure.

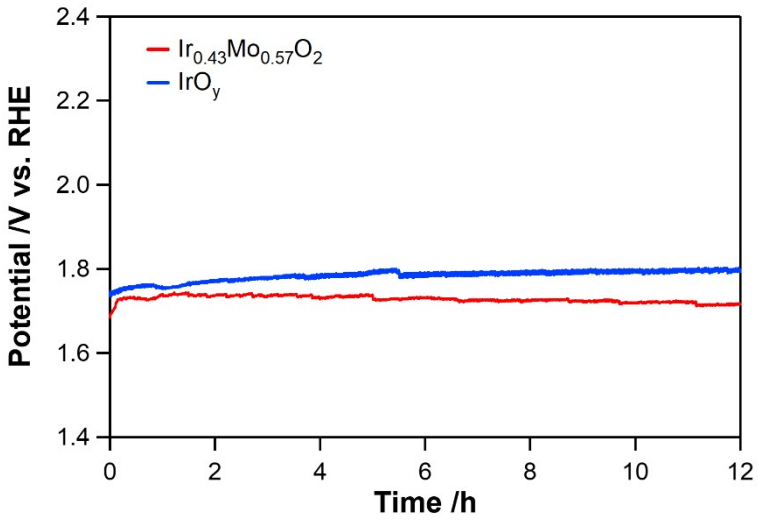

Fig. S13. Chronopotentiometric performances of $Ir_{0.43}Mo_{0.57}O_2$ and IrO_y under a constant current density of 10 mA cm^{-2} in 1 M NaCl (*aq*) for 12 h.

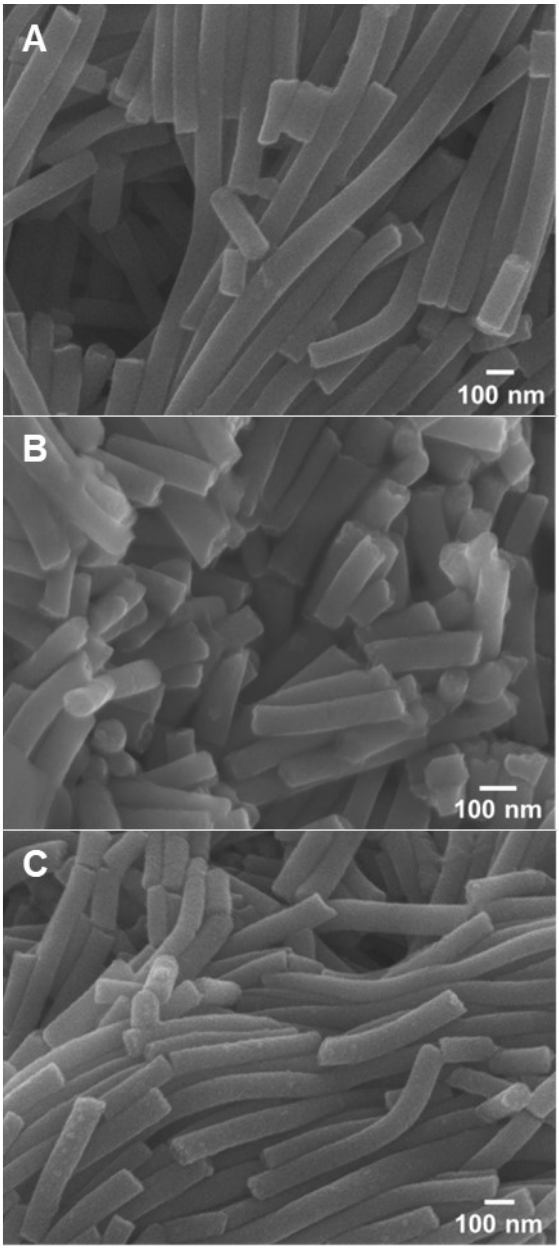

Fig. S14. SEM image of $Ir_{0.43}Mo_{0.57}O_2$ nanofibers after stability test for 12 h in (A) 1 M H_2SO_4, (B) 1 M PBS and (C) 1 M KOH solutions.

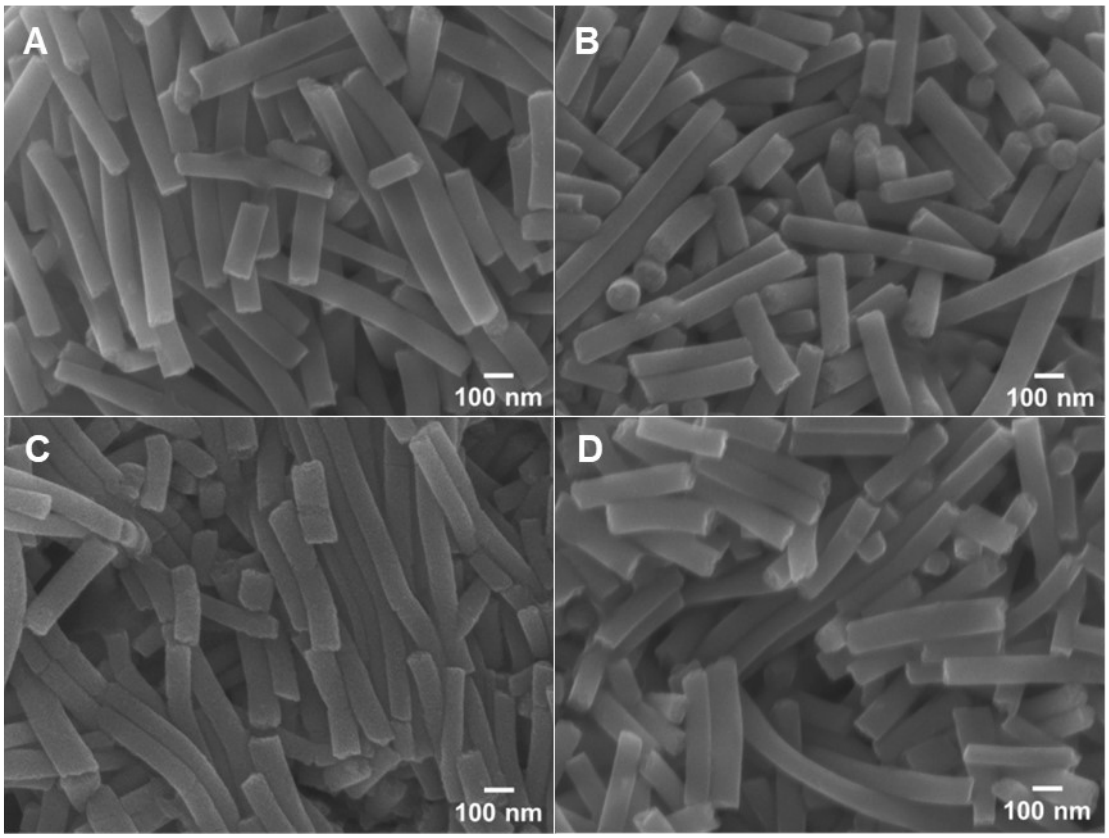

Fig. S15. SEM image of $Ir_{0.43}Mo_{0.57}O_2$ nanofibers after stability test for 12 h in (A,B) H_2SO_4 and (C,D) KOH solutions with different concentrations (A,C for 0.5 M; B,D for 0.1 M).

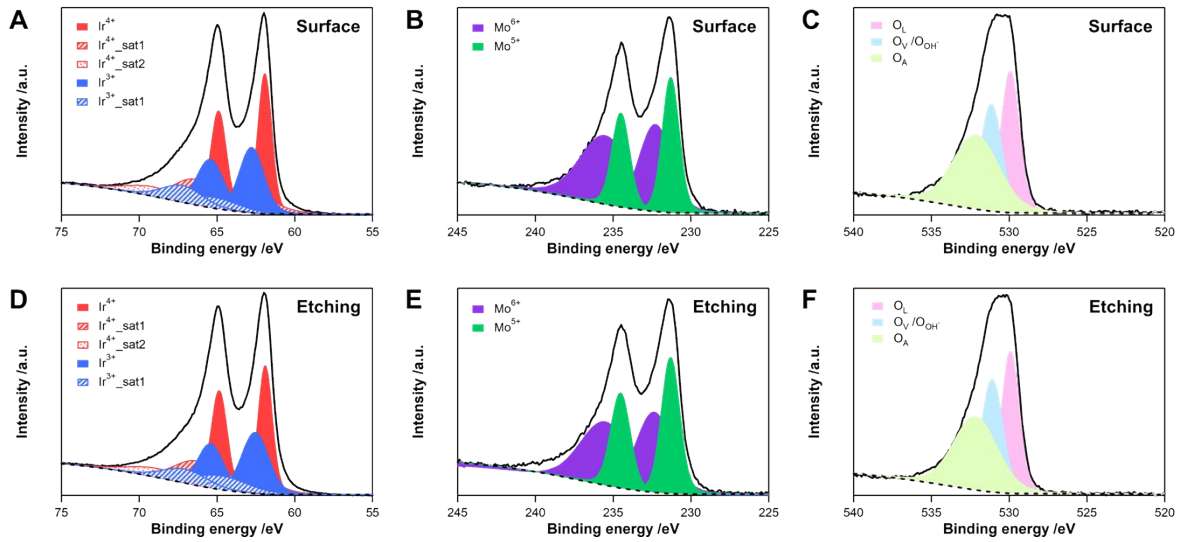

Fig. S16. Deconvoluted XPS core level spectra for (A,D) Ir 4f, (B,E) Mo 3d, (C,F) O 1s regions of $Ir_{0.43}Mo_{0.57}O_2$ obtained after stability test for 12 h in 1 M H_2SO_4. The spectra were collected for the material surface (A-C) before and (D-F) after etching for 5 seconds.

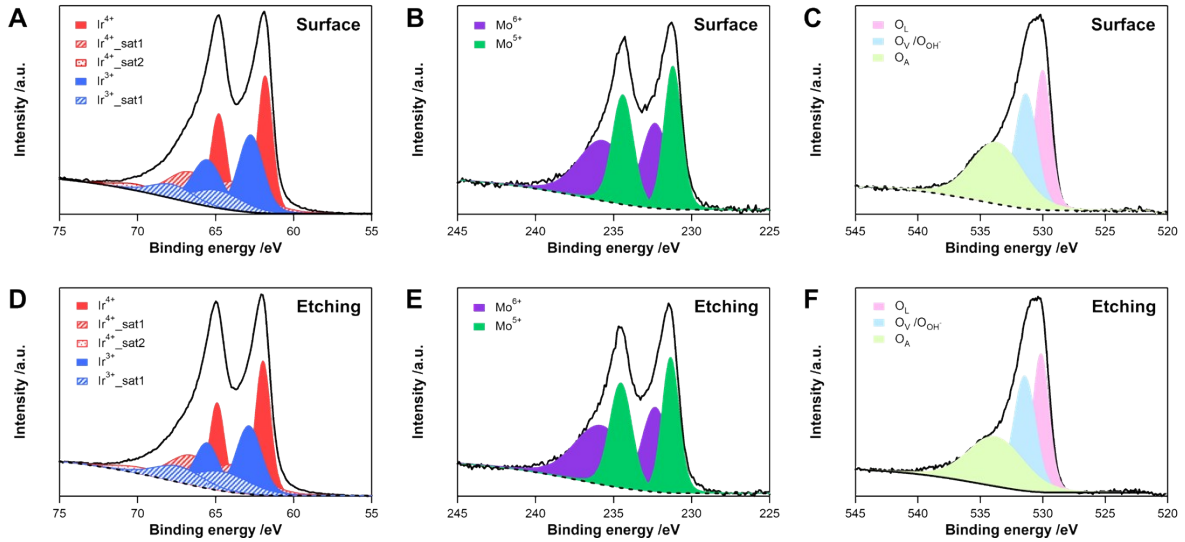

Fig. S17. Deconvoluted XPS core level spectra for (A,D) Ir 4f, (B,E) Mo 3d, (C,F) O 1s regions of $Ir_{0.43}Mo_{0.57}O_2$ obtained after stability test for 12 h in 1 M PBS (pH 7.1). The spectra were collected for the material surface (A-C) before and (D-F) after etching for 5 seconds.

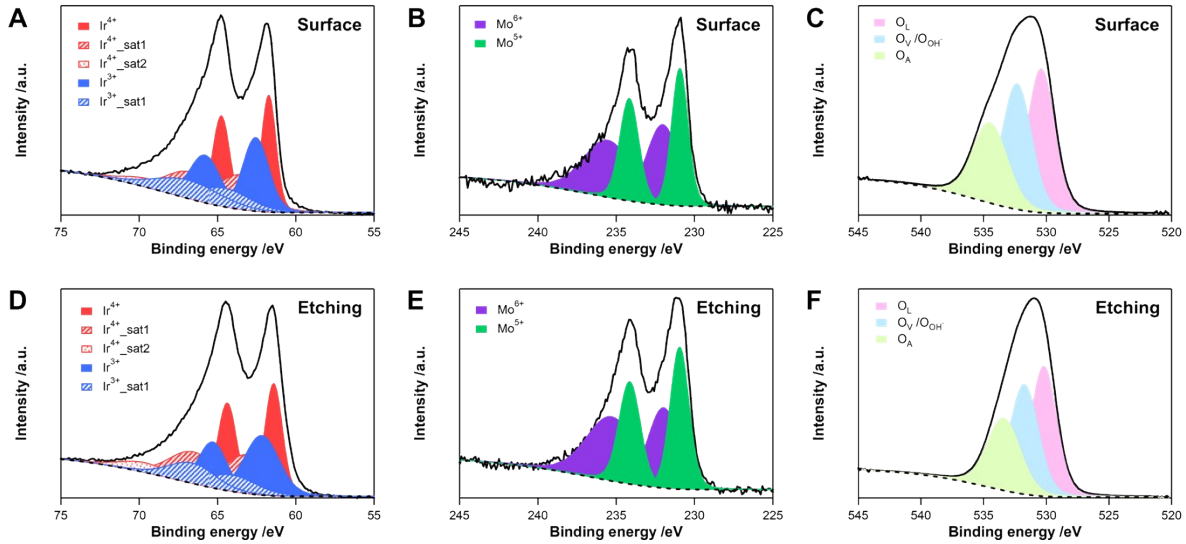

Fig. S18. Deconvoluted XPS core level spectra for (A,D) Ir 4f, (B,E) Mo 3d, (C,F) O 1s regions of $Ir_{0.43}Mo_{0.57}O_2$ obtained after stability test for 12 h in 1 M KOH. The spectra were collected for the material surface (A-C) before and (D-F) after etching for 5 seconds.